

## SANDQVIST 187: A DENSE MOLECULAR CLOUD IN NORMA

H. ALVAREZ,<sup>1</sup> L. BRONFMAN,<sup>1,2</sup> R. COHEN,<sup>2</sup> G. GARAY,<sup>3</sup> J. GRAHAM,<sup>3</sup> AND P. THADDEUS<sup>2,4</sup>

Received 1985 March 22; accepted 1985 July 10

## ABSTRACT

We present and discuss observations of Sandqvist 187, an elongated dust cloud in the southern constellation Norma. The cloud contains two Herbig-Haro objects, HH 56 and HH 57. HH 57 currently displays on its NE edge a 17th mag variable star of the FU Ori type. Using the Columbia University 1.2 m millimeter-wave telescope at Cerro Tololo, we have mapped the region and found an extended CO cloud which envelops and is elongated along the optical dust cloud. The position of maximum CO emission coincides with HH 56 and HH 57. Assuming a distance of 0.7 kpc, the total mass of the cloud is found to be close to  $500 M_{\odot}$ . The CO spectra show evidence of a molecular flow. Photographs and CCD images obtained mostly with the CTIO 4 m telescope show the detailed optical structure of the dark cloud's core region. The Herbig-Haro object HH 56 appears to be related to an emission-line star embedded in the small nebula Reipurth 13, not to the FU Ori Star in HH 57.

*Subject headings:* interstellar: molecules — nebulae: individual — stars: formation — stars: pre-main-sequence

## I. INTRODUCTION

Dense molecular gas clouds mark the sites of star formation within our own and other galaxies. The number and mass spectrum of the stars produced in a particular cloud can vary greatly. Large molecular clouds, where most stars originate, produce both high- and low-mass stars, but small clouds may produce only stars of low or intermediate mass. One example is ESO 210-6A, also known as Sandqvist 111 (Sandqvist 1977). This is a small cloud of  $7-15 M_{\odot}$  in which only a single star of low mass has apparently been able to form (Graham and Elias 1983; Emerson *et al.* 1984).

In a search for southern HH objects, Schwartz (1977) located two, HH 56 and HH 57, which appear to be connected with an isolated dark cloud cataloged as 187 in Sandqvist's survey. As seen on a direct photograph (Fig. 1), the cloud has an elongated appearance extending approximately  $38' \times 2'$ . The HH objects are located near the W extremity. During the last 2 yr, HH 57 has become the focus of attention following the flare-up of an FU Ori-type variable star on its NE edge. The star, which is very bright in the infrared, is clearly related to the HH 57 nebulosity. In the course of throwing off a high-velocity gaseous shell, it is injecting energy into its surrounding environment (Graham 1983; Cohen *et al.* 1984; Graham and Frogel 1985; Reipurth 1985). A search for and study of associated molecular gas was clearly appropriate, and we are reporting here on the significant enhancement of CO radiation observed in the area.

## II. OBSERVATIONS

We observed the 115 GHz CO line with the 1.2 m millimeter-wave telescope that Columbia University operates at Cerro Tololo Inter-American Observatory. The antenna has

a beamwidth of  $8.8$  (FWHM) at this frequency. The receiver and spectrometer were those used for the ongoing Columbia Southern Hemisphere galactic survey (Cohen 1983). The spectrometer was a 256 channel filterbank with a resolution of  $1.3 \text{ km s}^{-1}$ . Spectra were taken with a  $7.5$  separation on a grid oriented along galactic coordinates and centered on HH 57 itself (R.A.,  $16^{\text{h}}28^{\text{m}}57^{\text{s}}$ ; decl.,  $-44^{\circ}49'17''$  (1950);  $l$ ,  $338^{\circ}55$  and  $b$ ,  $+2^{\circ}12$ ). The grid points are shown as crosses in Figure 5. The integration time at each point, typically 12 minutes, was adjusted to give an rms noise of 0.1 K. The strong increase in CO intensity as the beam moves across the cloud can be appreciated from a series of measurements taken along the line of constant galactic latitude through HH 57 (Fig. 2).

A separate pair of observations was made to get low noise spectra at a point close to the maximum CO emission and in a comparison field one beamwidth away. For these we integrated a total of 340 minutes and 180 minutes, obtaining an rms noise of 0.015 K and 0.019 K, respectively. The HH 57 spectrum and the average off-peak spectrum are shown superposed in Figure 3. At the position of HH 57, the CO line is appreciably broadened. This we believe is due to gas flow near the cloud core (§ V). To evaluate the effects of saturation at the CO maximum, a measurement was made with the receiver tuned to the  $^{13}\text{CO}$  line at 110.20 GHz. The profile is shown as Figure 4, and the observation discussed in § IV.

At each gridpoint in Figure 5 we measured the peak velocity (with respect to local standard of rest) and the antenna temperature integrated over velocity from  $-11.7$  to  $+5.2 \text{ km s}^{-1}$ . In Figure 5, the results are shown in contour map form superposed on a photograph of the field.

## III. GENERAL CHARACTERISTICS AND MORPHOLOGY OF THE CLOUD

Figure 5 shows that the molecular cloud in CO is elongated and extends along the optical image of the dark nebula. To within one-half beamwidth, the strongest CO radiation comes from the region of HH 57; the second HH object, HH 56, is only  $50''$  NW of HH 57 and also falls inside a beam centered on HH 57. The average velocity (LSR) of the CO peak is

<sup>1</sup> Universidad de Chile.<sup>2</sup> Columbia University.<sup>3</sup> National Optical Astronomy Observatories-Cerro Tololo Inter-American Observatory, operated by the Association of Universities for Research in Astronomy, Inc., under contract with the National Science Foundation.<sup>4</sup> Goddard Institute for Space Studies.

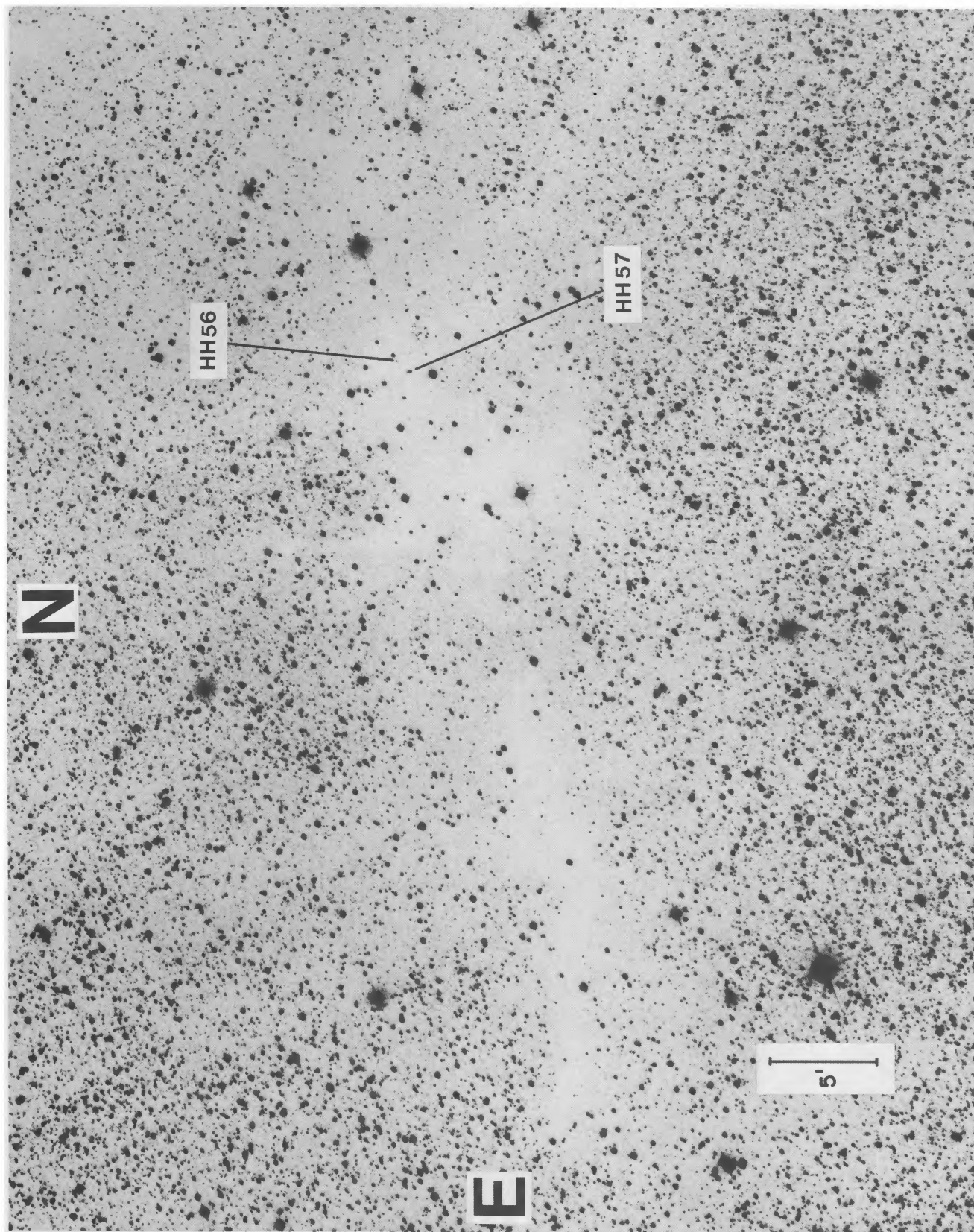


FIG. 1.—The Sandqvist 187 cloud. This photograph was taken by P. Boscolo on 1984 April 2 with the Curtis Schmidt telescope of the University of Michigan at CTIO. The emulsion was IIIa-J, and a GG385 filter was used with exposure 60 minutes. HH 56 and HH 57 are marked.

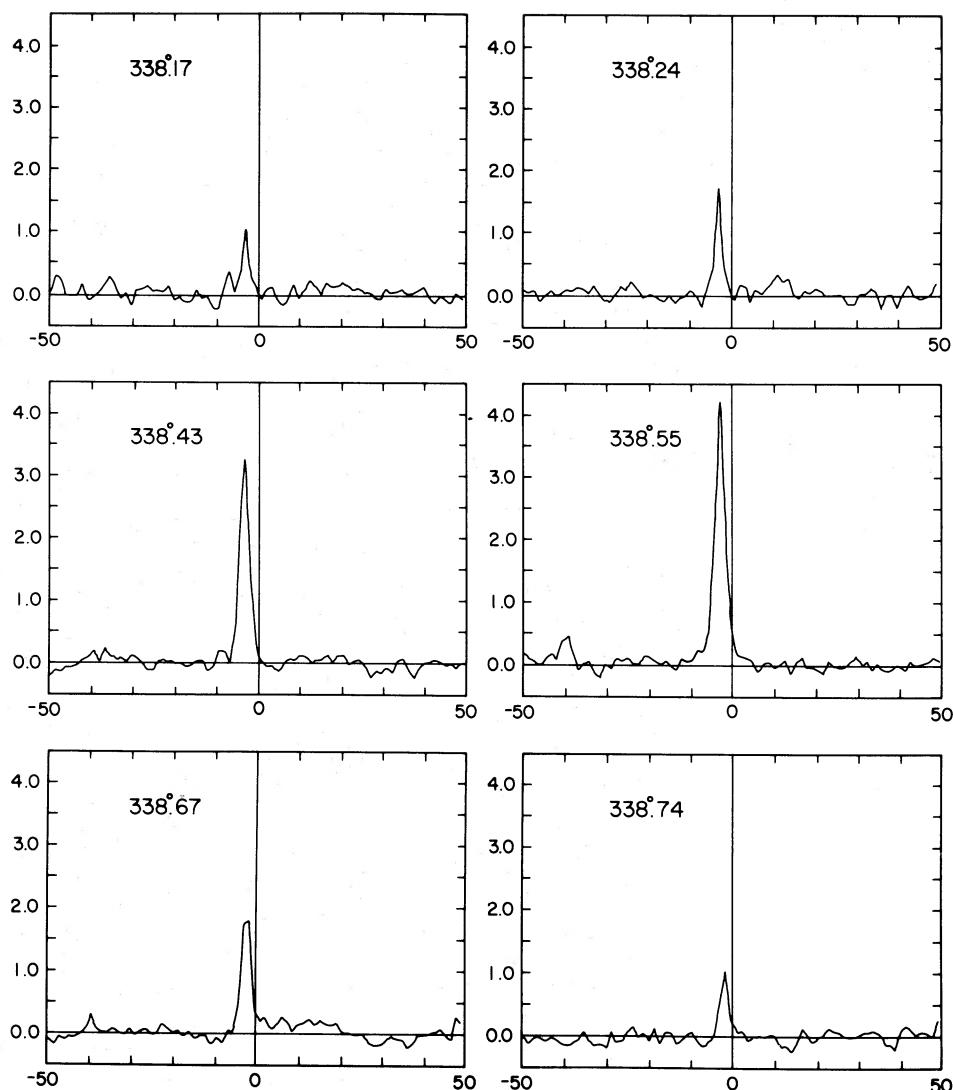


FIG. 2.—Sample CO profiles toward the Norma cloud, along a line of constant galactic latitude  $b = 2^{\circ}12$  passing through HH 57. In each frame, antenna temperature  $T_A$  (K) (ordinate) is plotted against velocity ( $\text{km s}^{-1}$ ) (abscissa). Note the sharp peak in the signal at the position of HH 57 ( $l = 338^{\circ}55$ ).

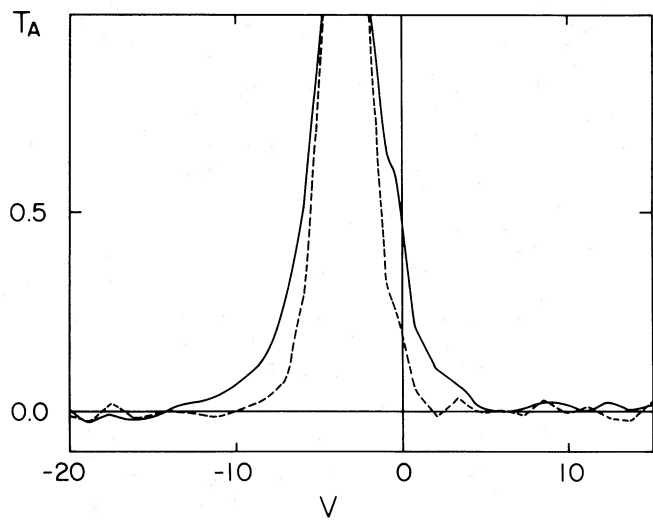


FIG. 3

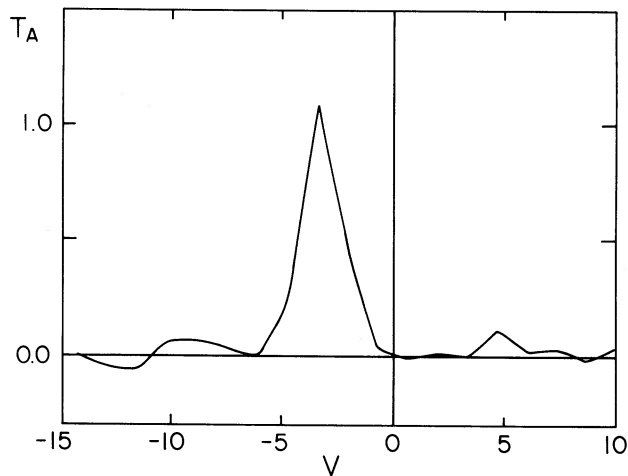


FIG. 4

FIG. 3.—CO profiles with long integration times. These were made with the beam at the HH 57 position  $l = 338^{\circ}55$ ,  $b = 2^{\circ}04$  (continuous curve) and at one beamwidth distant ( $l = 338^{\circ}67$ ,  $b = 1^{\circ}99$ ) (dashed curve). They show significant line broadening in the beam which includes the HH regions and the embedded stars.

FIG. 4.—Line emission by  $^{13}\text{CO}$  toward HH 57 with an integration time of 21 minutes.

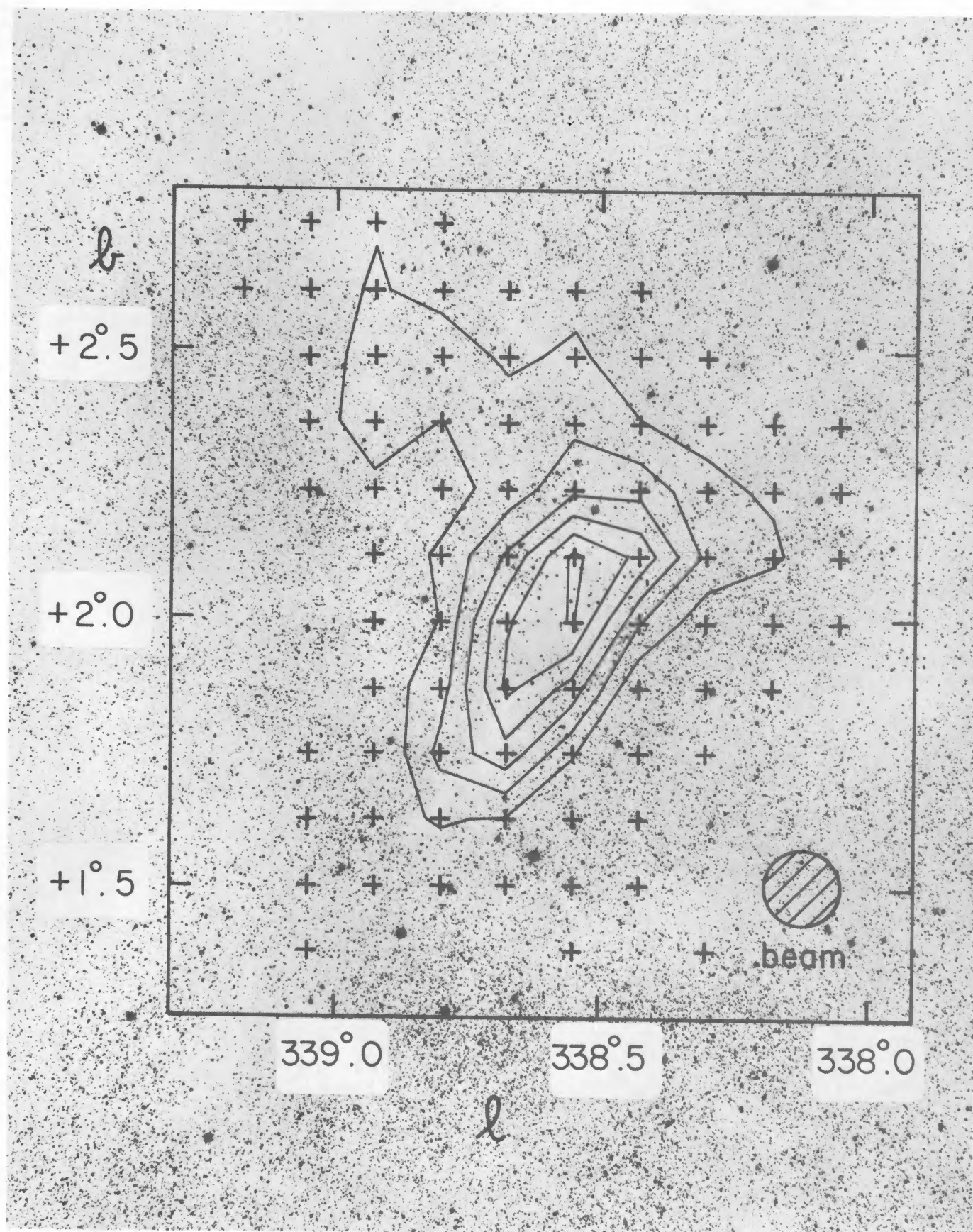


FIG. 5.—Map of CO line emission from the Norma cloud. The contours are superposed on the Fig. 1 photograph which is this time oriented along galactic coordinates. Contours are spaced every 2 units up to the maximum of  $12 \text{ K km s}^{-1}$ . The crosses indicate the positions where observations were made. The upper cross on the central contour coincides with the HH 57 position.

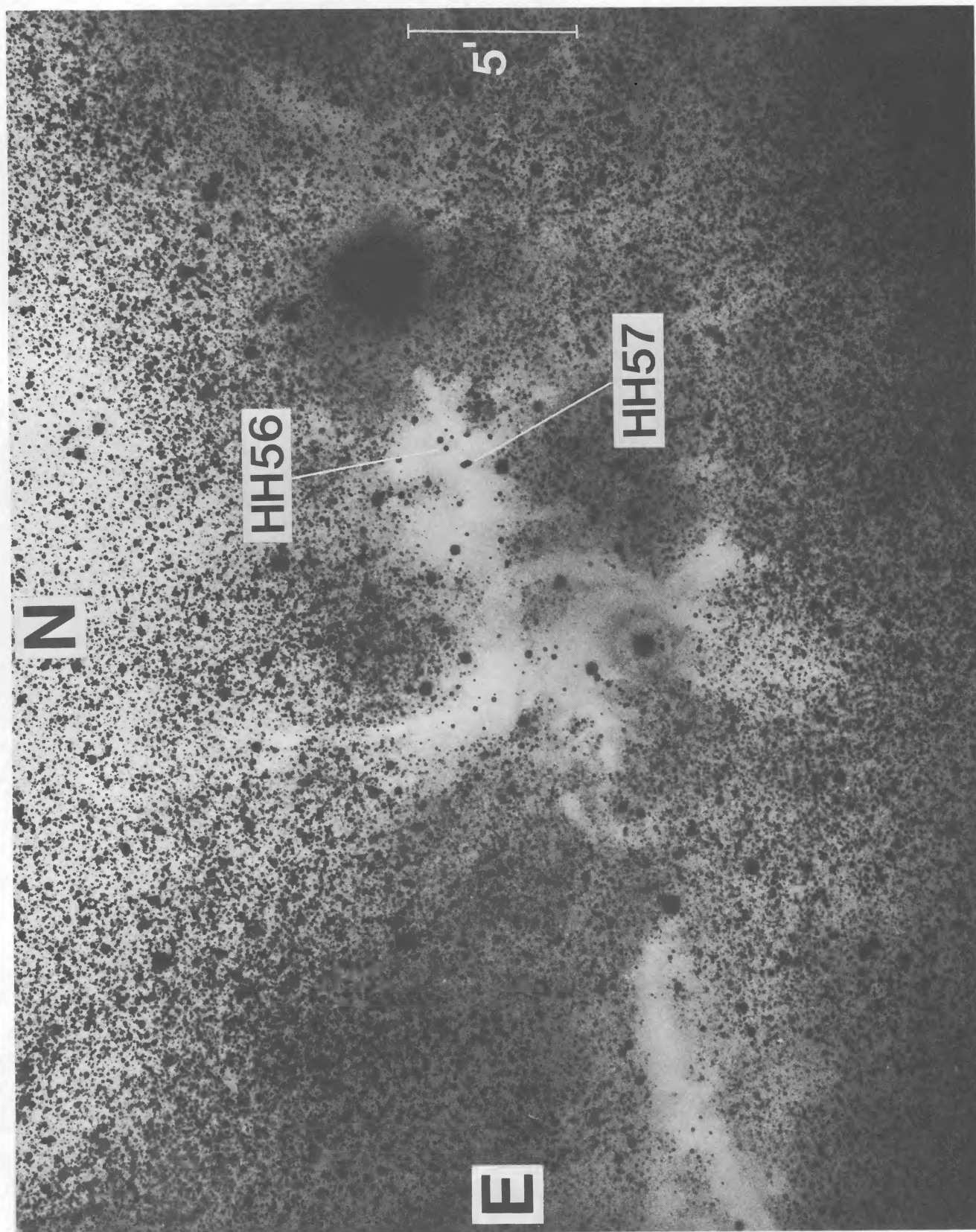


FIG. 6.—A contrast-enhanced photograph of Sandqvist 187. The original plate was taken on 1983 June 8, with the CTIO 4 m telescope using IIIa-F emulsion and an OG570 filter. The exposure time was 15 minutes.

$-3.8 \pm 0.8 \text{ km s}^{-1}$ , and there is no noticeable velocity gradient along the cloud. Graham and Frogel (1985) estimate a distance of 0.7 kpc, but this is uncertain to about 50%. In addition to the dominant line peaking at  $-3.8 \text{ km s}^{-1}$ , some spectra show weak lines ( $T_{\text{peak}} \approx 0.5 \text{ K}$  near  $-40$  and  $-70 \text{ km s}^{-1}$ ). These features persist as the telescope is directed away from the molecular cloud toward the galactic plane. Almost certainly they correspond to more distant molecular gas in the outer parts of the Galaxy.

Within the overall filamentary shape of the Sandqvist 187 cloud, images obtained with the CTIO 4 m telescope show abundant fine structure which is beyond the resolution of the CO telescope. Figure 6 shows a contrast-enhanced negative image taken from a prime focus photograph in orange-red light. This photograph registers stars much fainter than Figure 1 enabling us to penetrate the lighter areas of absorption. Note, for example, how the filamentary nebula is divided about halfway along its length by a lane where the absorption is comparatively low. The densest obscuring dust concentrates along a ridge which forms a central axis of the dark cloud. It can be seen in Figure 5 that, even allowing for the difference in angular resolution of the optical and radio data, the CO extends far beyond this central ridge.

Figure 7 shows a still deeper penetration into the heart of the nebula. This image is from a 20 minute CCD exposure, taken with the 4 m prime focus CCD camera through a filter giving an effective bandpass of  $0.7\text{--}1.1 \mu\text{m}$ . The bright stars in this frame show saturation effects leading to image overflow into the pixel rows on the left. Some fringing remains from incomplete removal of interference fringes in the chip caused by night sky lines in the near-infrared. Comparing Figures 6 and 7, one notices several very red stars shining through the dust. None except the HH 57 star are bright in the far-infrared, so all are probably background objects. The brightest of these may prove useful for mapping polarization produced by anisotropic scattering from the dust in the cloud.

The core of the dust cloud is shown most clearly by a computer-enhanced plot (Fig. 8) which also serves as a key for Figure 7. Figure 8 is made from the same CCD frame as Figure 7, but here only those pixels with an accumulated count less than a threshold of 5880 counts are marked by a black dot. The dots thus indicate the darkest part of the nebula. From an examination of Figures 7 and 8, two features should be noted.

1. Dense knots of dust and presumably molecular gas are located near the optical features HH 56, HH 57, and the small luminous nebula Reipurth 13 (Reipurth 1981). However, HH 56 appears to lie in or near a comparatively clear window where a few background stars do shine through in the near infrared.

2. The filamentary form of the cloud core is remarkably similar to the outer contours of the cloud as seen on wide field photographs (e.g., Fig. 1). This suggests that, in the course of the formation of the core, the overall shape is preserved. Figures 7 and 8 show cloud structure on scale of the order of  $10''$  in the area around HH 56 and HH 57. At a distance of 700 pc, this corresponds to a linear dimension of 0.03 pc.

#### IV. EXCITATION TEMPERATURE, COLUMN DENSITY, AND CLOUD MASS

The excitation temperature and  $\text{H}_2$  column density were obtained using the  $^{12}\text{CO}$  and  $^{13}\text{CO}$  data at the position of the cloud core. For the calculation, we assume local thermodynamic equilibrium and a large optical depth for the  $^{12}\text{CO}$  line (cf.

Spitzer 1978). From the observed antenna temperatures

$$T_A(^{12}\text{CO}) = 4.2 \pm 0.1 \text{ K}$$

and

$$T_A(^{13}\text{CO}) = 1.3 \pm 0.1 \text{ K}$$

and the  $^{13}\text{CO}$  line width

$$\Delta V(^{13}\text{CO}) = 2.2 \pm 0.4 \text{ K km s}^{-1} \text{ (FWHM)},$$

we find

$$T_x = 7.5 \text{ K} \text{ (excitation temperature)},$$

$$\tau(^{13}\text{CO}) = 0.37 \text{ (}^{13}\text{CO optical depth)},$$

$$N(^{13}\text{CO}) = 2.8 \times 10^{15} \text{ cm}^{-2} \text{ (}^{13}\text{CO column density)},$$

and

$$N(\text{H}_2) = 1.4 \times 10^{21} \text{ cm}^{-2} \text{ (H}_2 \text{ column density)}.$$

The derived molecular hydrogen column density assumes a  $N(^{13}\text{CO})$  to  $N(\text{H}_2)$  ratio of  $2 \times 10^{-6}$  (Dickman 1978).

Finally, using observed major and minor extents of 33' and 14' for the cloud and assuming a distance of 0.7 kpc, we estimate a total mass of  $500 M_\odot$ . In this calculation we use a mean molecular weight per  $\text{H}_2$  molecule of  $4.0 \times 10^{-24} \text{ g}$  (which assumes 1 He atom for every five  $\text{H}_2$  molecules).

#### V. THE EVIDENCE FOR A MOLECULAR FLOW

Outflows of molecular gas frequently accompany regions of star formation. They are often related to individual embedded stars, and the flows are parallel to the motions of associated HH objects. Strong stellar winds originating near the surfaces of the stars probably provide the energy (Bally and Lada 1983; Edwards and Snell 1983). Detection of flows is not easy with an 8'8 beam since the outflows often extend only over 1' or 2' (Rodríguez *et al.* 1982). The antenna temperature of the high-velocity gas is thus greatly reduced by beam dilution, and careful observation is required to detect the flow, but there is evidence for such a phenomenon in our data.

Figure 3 shows the CO spectrum at the position of HH 57 ( $l = 338.5$ ,  $b = 2.12$ ), and Table 1 gives the observed antenna temperature in all channels with emission above  $3\sigma$  where  $\sigma$  is the rms noise temperature. The profile has a full width of  $2.9 \text{ km s}^{-1}$  at half-intensity, and a full width of  $11.4 \text{ km s}^{-1}$  at the 0.1 K level. A single Gaussian line having the same peak antenna temperature and FWHM would have a full width of about  $7 \text{ km s}^{-1}$  at the 0.1 K level. At a position one beam-

TABLE 1  
HH 57 PROFILE

Channel	Central Velocity ( $\text{km s}^{-1}$ )	Antenna Temperature (K)
-9.75.....		$0.07 \pm 0.02$
-8.45.....		0.12
-7.15.....		0.25
-5.85.....		0.49
-4.55.....		2.17
-3.25.....		4.23
-1.95.....		2.48
-0.65.....		0.61
0.65.....		0.21
1.95.....		0.10
3.25.....		0.06

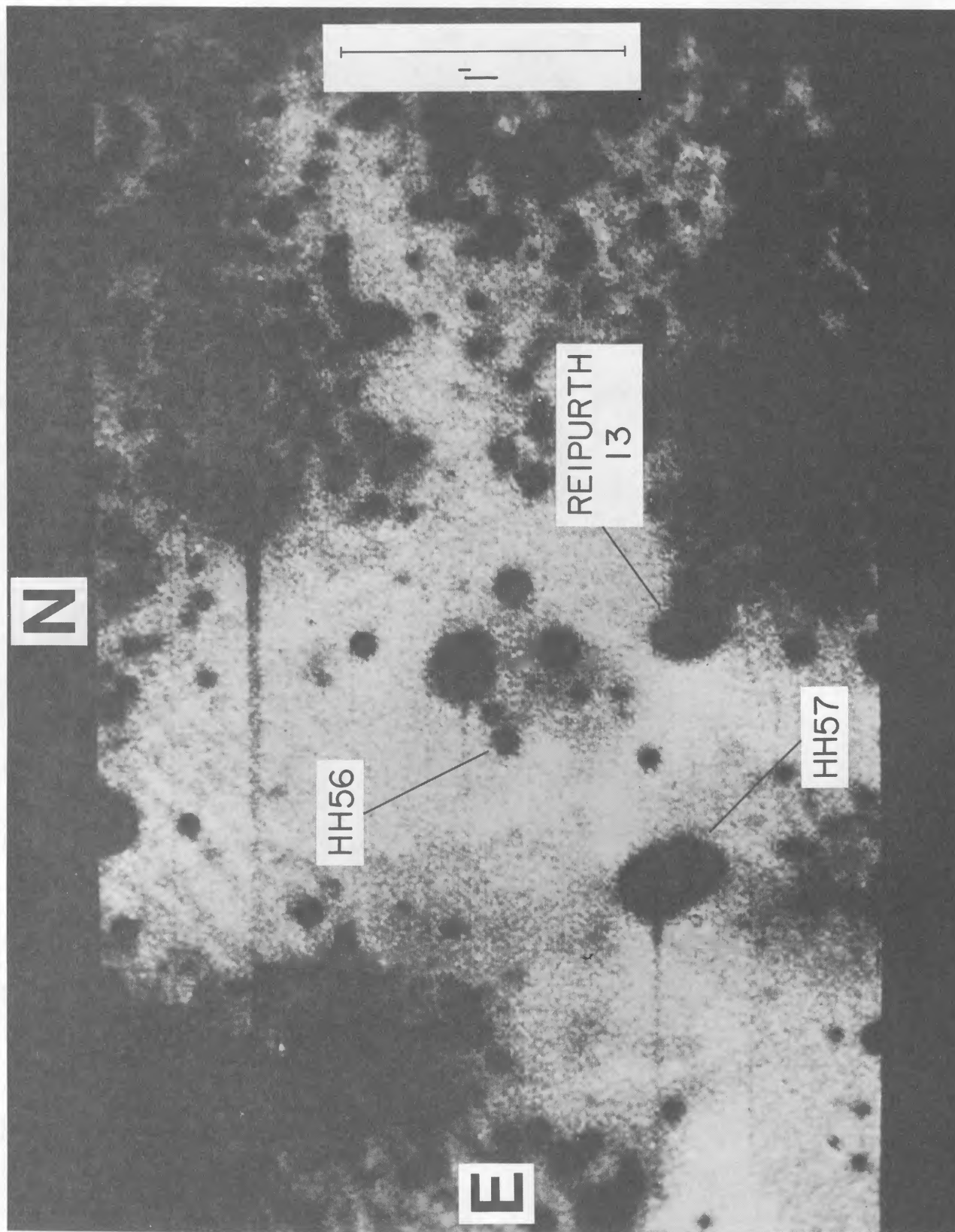


FIG. 7.—CCD frame of the cloud core in the near-infrared, taken with the CTIO 4 m telescope and prime focus CCD camera on 1983 October 10. The bandpass, determined by the cut-off of an RG695 filter and the sensitivity limit of the RCA chip, is approximately  $0.7\text{--}1.0\ \mu\text{m}$ . Note the general clumpy, uneven appearance of the densest part of the cloud. Several very red stars which are not seen in Fig. 6 are recorded. These are presumably background stars heavily reddened by the dust in the nebula.

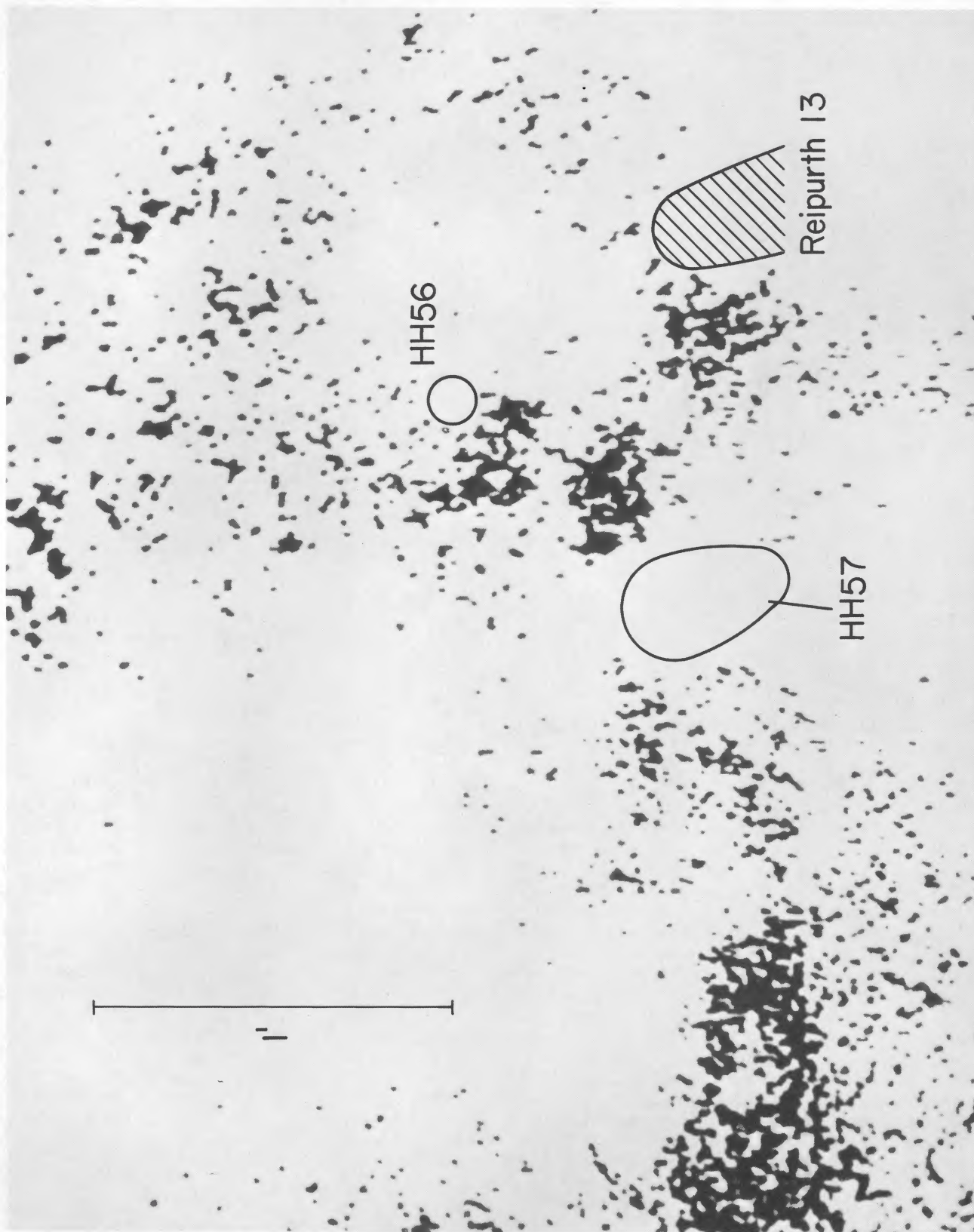


FIG. 8.—Computer enhancement of Fig. 7. This shows, as black dots, the optically darkest regions in Sandqvist 187.

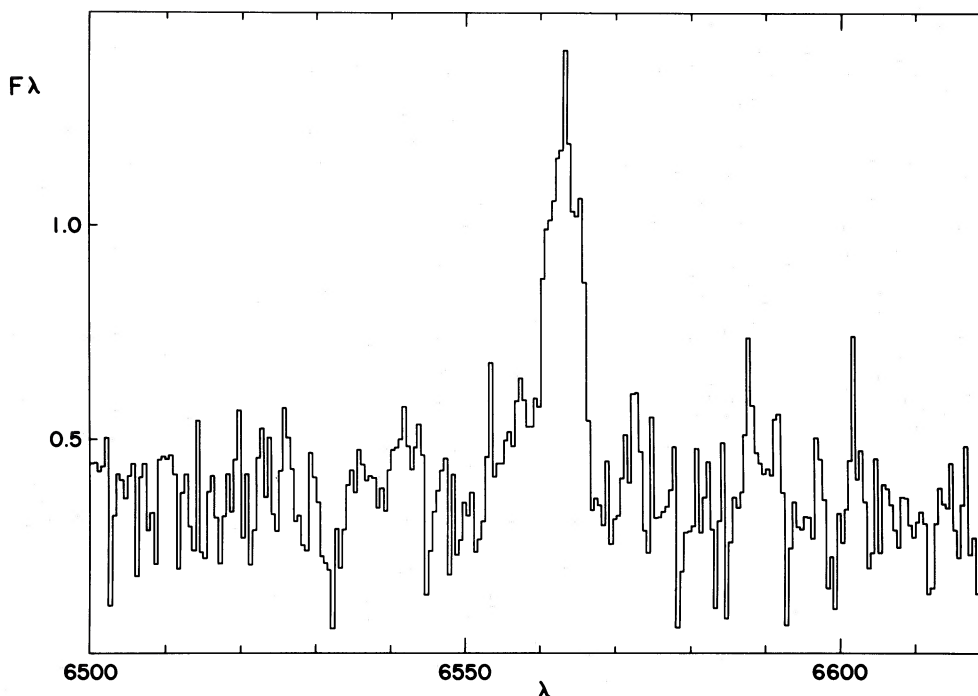


FIG. 9.—The spectrum of Reipurth 13 near  $H\alpha$ . This is taken from a scan made on 1984 June 7 with the CTIO 4 m telescope and Cassegrain spectrograph. Strong, broad  $H\alpha$  line emission is superposed on a weak continuum. Flux is in relative units.

width from HH 57, the profile has approximately the same antenna temperature and FWHM (3.88 K and  $2.8 \text{ km s}^{-1}$ , respectively). The line width at the 0.1 K level, though, changes to  $7.7 \text{ km s}^{-1}$ . This suggests that the wing emission, which is confined to one beamwidth, arises from a molecular outflow related to the HH 57 object.

Further observation with a smaller beam is clearly desirable. Here the situation may be complicated by a second embedded stellar object in the area lying within or close to the small nebula Reipurth 13. A spectrum taken with the CTIO 4 m telescope (Fig. 9) shows that while Reipurth 13 shines mostly in continuum light, it also has a broad  $H\alpha$  emission component ( $\sim 200 \text{ km s}^{-1}$  FWHM) near zero velocity ( $-9 \text{ km s}^{-1}$ ) which persists after a careful subtraction of background sky radiation from the surroundings. The equivalent width of this line is  $12 \text{ \AA}$  in continuum units. This spectrum suggests that a young star with an active chromosphere is illuminating the nebula. No infrared source has been identified here (Cohen *et al.* 1984), but it would be worthwhile to push the search to higher sensitivity levels. The Reipurth 13 object may be responsible for HH 56 which is otherwise difficult to account for with the proposed geometry for HH 57 and its star. HH 56 has a positive velocity of  $+36 \text{ km s}^{-1}$  (Schwartz and Dopita 1980) and is located in a relatively transparent area of the dark cloud where several background stars can be seen (Fig. 7); it may thus be on the far side of Reipurth 13 and receding from both us and the embedded star. Such a geometry is also suggested by the significant proper motion vector of HH 56 measured by

Schwartz, Jones, and Sirk (1984). This is directed away from Reipurth 13 and could mark the presence of a second material flow in the region approximately parallel to that powered by the HH 57 star.

#### VI. CONCLUDING REMARKS

We have shown in this paper that a well-defined CO cloud coincides with the dust cloud, Sandqvist 187, where star formation is currently taking place. The contours of the CO radiation follow closely the optical cloud with the maximum CO emission and the highest concentration of dust occurring at the actual site of the young, recently created stars. In this cloud core, optical structure as small as  $0.03 \text{ pc}$  is observed. Evidence for molecular flows is seen. For the entire cloud, we estimate a mass of  $500 M_{\odot}$ .

Clearly the Sandqvist 187 cloud holds great promise for narrow-beam observations in the millimeter-wave region when the appropriate instrumentation becomes available in the southern hemisphere. High-resolution infrared techniques as well could be applied with profit to the strong source associated with the HH 57 star. We emphasize that, in this type of study, there is an essential complementarity between the optical, infrared, and millimeter-wave observations. When all are brought together, it becomes possible to understand far more about the nature of the molecular clouds and the star forming process than can ever be achieved with any one technique on its own.

#### REFERENCES

- Bally, J., and Lada, C. J. 1983, *Ap. J.*, **265**, 824.  
 Cohen, R. S. 1983, in *Surveys of the Southern Galaxy*, ed. W. B. Burton and F. P. Israel (Dordrecht: Reidel), p. 264.  
 Cohen, M., Schwartz, R. D., Harvey, P. M., and Wilking, B. A. 1984, *Ap. J.*, **281**, 250.  
 Dickman, R. L. 1978, *Ap. J. Suppl.*, **37**, 407.  
 Edwards, S., and Snell, R. L. 1983, *Ap. J.*, **270**, 605.  
 Emerson, J. P., Harris, S., Jennings, R. E., Beichman, C. A., Baud, B., Beintema, D. A., Marsden, P. L., and Wesselius, P. R. 1984, *Ap. J. (Letters)*, **278**, L49.  
 Graham, J. A. 1983, *IAU Circular*, 3785.  
 Graham, J. A., and Elias, J. H. 1983, *Ap. J.*, **272**, 615.  
 Graham, J. A., and Frogel, J. A. 1985, *Ap. J.*, **289**, 331.

Reipurth, B. 1981, *Astr. Ap. Suppl.*, **44**, 379.  
———. 1985, *Astr. Ap.*, **143**, 435.

Rodríguez, L. F., Carral, P., Ho, P. T. P., and Moran, J. M. 1982, *Ap. J.*, **260**, 635.

Sandqvist, A. 1977, *Astr. Ap.*, **57**, 467.

Schwartz, R. D. 1977, *Ap. J. Suppl.*, **35**, 161.

Schwartz, R. D., and Dopita, M. A. 1980, *Ap. J.*, **236**, 543.

Schwartz, R. D., Jones, B. F., and Sirk, M. 1984, *A.J.*, **89**, 1735.

Spitzer, L., Jr. 1978, in *Physical Processes in the Interstellar Medium* (New York: J. Wiley), p. 8.

H. ALVAREZ: Department of Astronomy, University of Chile, Casilla 36-D, Santiago, Chile

L. BRONFMAN, R. COHEN, and P. THADDEUS: Goddard Institute for Space Studies, 2880 Broadway, New York, NY 10025

G. GARAY: European Southern Observatory, Karl-Schwarzschild-Strasse 2, D-8046 Garching bei Munchen, Federal Republic of Germany

J. A. GRAHAM: Carnegie Institution of Washington, Department of Terrestrial Magnetism, 5241 Broad Branch Road, N.W., Washington, DC 20015